Proton NMR Characterization of the Catalytically Relevant Proximal and Distal Hydrogen-Bonding Networks in Ligated Resting State Horseradish Peroxidase

V. Thanabal,[1a] Jeffrey S. de Ropp,[1b] and Gerd N. La Mar*[1a]

Contribution from the Department of Chemistry and the University of California, Davis, NMR Facility, University of California, Davis, California 95616. *Received September 22, 1987*

Abstract: Proton NMR spectroscopy of the low-spin cyanide complex of horseradish peroxidase, HRPCN, in H_2O solution was used to examine exchangeable resonances of functionally important amino acids in the heme pocket and their role in hydrogen-bonding networks, which have been proposed to facilitate peroxidase catalysis. Spectra were analyzed by use of nuclear Overhauser effect and saturation-transfer spectroscopies, along with consideration of paramagnetic shift and relaxation. Definitive assignments could be made in spite of the size of the proteins (42 kDa), its inherent paramagnetism (iron(III), $S = {}^1/_2$), and the relatively few resolved resonances, suggesting that these NMR methods may be applicable to even larger heme proteins. The resonance identification was made for labile protons of the proximal His-170, distal His-42, and a heme peripheral contact, Tyr-185, which confirm the close similarity of the heme pocket stereochemistry of horseradish and cytochrome *c* peroxidases. The resonance assignments enabled determination of several key facets of the structure of the heme cavity of HRPCN. The proton taken up in concert with anionic ligand binding is shown to be present on the His-42 imidazole ring, forming a imidazolium side chain that hydrogen bonds sufficiently strongly to the nitrogen of the bound cyanide to induce a detectable isotope effect on the electronic structure of the heme. The strength of the hydrogen bond is confirmed by the stability of this network over the pH range 4-11. The labile ring proton of the proximal His-170 in HRPCN was located in a position that is consistent with an imidazolate description of the axial ligand but with the proton transferred to a nearby amino acid acceptor site less than 1 Å removed. The structural changes in the heme and proximal and distal amino acid residues upon ligand binding is discussed as a model for HRP compound II formation.

Heme proteins display highly diverse biological functions while retaining an essentially unaltered prosthetic group consisting of an iron bound to protoporphyrin IX (Figure 1). Therefore the nature of the side chains of the folded polypeptide matrix and their interaction with the heme and its substrate control the reactivity of the iron center.[2,3] Horseradish peroxidase, HRP, is an example of a wide class of plant heme proteins involved in bacterial defense, which decomposes H_2O_2 at the expense of aromatic donors.[4,5] Several similar classes of peroxidases occur in yeast and mammals.[5] The X-ray single-crystal structure of yeast cytochrome *c* peroxidase, *Cc*P, has been reported.[6,7] These heme peroxidases exhibit in common the feature that they effect the heterolytic cleavage of the O-O bond in peroxides, with the result that the enzyme is raised two oxidizing equivalents above the resting state. Various specific properties of these proteins have been proposed[6,7] to facilitate this process. They involve hydrogen-bonding networks on both the proximal and distal side of the heme that stabilize the higher oxidation states of iron in compounds I and II by imparting significant imidazolate character to the axially bound histidine and provide a catalytic pocket in the distal side consisting of an Arg and His for the binding and cleavage of H_2O_2. The functional role of these residues has been discussed in detail for *Cc*P and proposed as general features of peroxidases.[6,7]

In the absence of a X-ray structure of HRP, considerable emphasis has been placed on the use of spectroscopic techniques[8-19] and the sequence homology to *Cc*P relevant to the active site.[20,21] Prominent among the spectroscopic methods has been the use of NMR spectroscopy.[10-19] The large hyperfine shifts for the heme and nearby amino acid residues permit resolution of their resonances[22,23] and thereby allow focus on only the vicinity of the heme cavity in this large enzyme. The ligated state of HRP is conveniently modeled by the low-spin cyano complex, HRPCN. It provides, in addition to conveniently narrow resonances with significant spectral dispersion, a magnetic dipole field due to the anisotropy[18,24] of the iron center, which imparts dipolar hyperfine shifts to a significant number of the amino acid side chain protons, thereby allowing their resolution, assignment, and eventual interpretation of the shift in terms of detailed stereochemistry.[18,19]

We have embarked on a comprehensive ^1H NMR study of the molecular structure and catalytic activity of HRPCN using a variety of techniques such as isotope labeling,[13] iron-induced differential dipolar relaxation,[18,19] nuclear Overhauser effects[17-19] (NOE), and saturation transfer spectroscopy.[18,19] The study is aimed at a detailed characterization of the electronic and magnetic

* Address correspondence to: Professor Gerd N. La Mar, Department of Chemistry, University of California, Davis, California 95616.

(1) (a) Department of Chemistry. (b) UCD NMR Facility.
(2) Antonini, E.; Brunori, M. In *Hemoglobin and Myoglobin in Their Reactions with Ligands*; Elsevier: New York, 1971.
(3) Saunders, B. C. In *Inorganic Biochemistry*; Eichhorn, G. L., Ed.; Elsevier: Amsterdam, 1973; Vol. 2, pp 988-1021.
(4) Dunford, H. B. *Adv. Inorg. Biochem.* **1982**, *4*, 41-68.
(5) Dunford, H. B.; Stillman, J. S. *Coord. Chem. Rev.* **1976**, *19*, 187-251.
(6) Poulos, T. L.; Kraut, J. *J. Biol. Chem.* **1980**, *255*, 8199-8205.
(7) Finzel, B. C.; Poulos, T. L.; Kraut, J. *J. Biol. Chem.* **1984**, *259*, 13027-13036.
(8) Colvin, J. T.; Rutter, R.; Stapleton, H. J.; Hager, L. P. *Biophys. J.* **1983**, *41*, 105-108.
(9) Nozawa, T.; Kobayashi, N.; Hatano, M.; Ueda, M.; Sogami, M. *Biochim. Biophys. Acta* **1980**, *626*, 282-290.
(10) Callahan, P. M.; Bobcock, G. T. *Biochemistry* **1981**, *20*, 952-958.
(11) La Mar, G. N.; de Ropp, J. S.; Smith, K. M.; Langry, K. C. *J. Biol. Chem.* **1980**, *225*, 6646-6652.
(12) La Mar, G. N.; de Ropp, J. S.; Smith, K. M.; Langry, K. C. *J. Biol. Chem.* **1981**, *256*, 237-243.
(13) De Ropp, J. S.; La Mar, G. N.; Smith, K. M.; Langry, K. C. *J. Am. Chem. Soc.* **1984**, *106*, 4438-4444.
(14) La Mar, G. N.; de Ropp, J. S. *J. Am. Chem. Soc.* **1982**, *104*, 5203-5206.
(15) Morishima, I.; Ogawa, S.; Inubushi, T.; Yonezawa, T.; Iizuka, T. *Biochemistry* **1977**, *16*, 5109-5115.
(16) Williams, R. J. P.; Wright, P. E.; Mazza, G.; Ricard, J. R. *Biochim. Biophys. Acta* **1975**, *581*, 127-147.
(17) Thanabal, V.; de Ropp, J. S.; La Mar, G. N. *J. Am. Chem. Soc.* **1986**, *108*, 4244-4245.
(18) Thanabal, V.; de Ropp, J. S.; La Mar, G. N. *J. Am. Chem. Soc.* **1987**, *109*, 265-272.
(19) Thanabal, V.; de Ropp, J. S.; La Mar, G. N. *J. Am. Chem. Soc.*, in press.
(20) Welinder, K. G. *Eur. J. Biochem.* **1985**, *151*, 497-504.
(21) Sakurada, J.; Takahashi, S.; Hosoya, T. *J. Biol. Chem.* **1986**, *261*, 9657-9662.
(22) La Mar, G. N. In *Biological Application of Magnetic Resonance*; Shulman, R. G., Ed.; Academic: New York, 1979; pp 305-343.
(23) Satterlee, J. D. *Annu. Rep. NMR Spectrosc.* **1986**, *17*, 79-178.
(24) Blumberg, W. E.; Peisach, J.; Wittenberg, B. A.; Wittenberg, J. B. *J. Biol. Chem.* **1968**, *43*, 1854-1862.

0002-7863/88/1510-3027$01.50/0

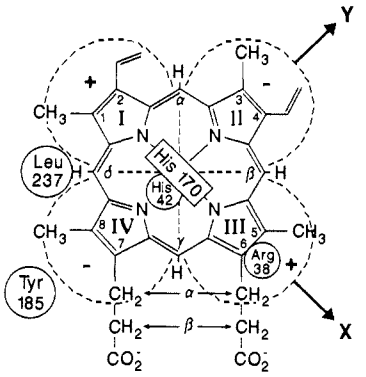

Figure 1. Structure and numbering system for hemin in HRPCN. The in-plane magnetic X and Y axes are shown, with the orientation of the proximal histidine (His-170) imidazole plane along the X axis.[18,19] The disposition of other amino acid residues in the heme cavity is shown such that large and small circles indicate amino acid residues on the proximal and distal side.[20,21] The rhombic magnetic anisotropy yields a cloverleaf-shaped distribution of dipolar shift with the upfield shifts given as positive and the downfield shift as negative.[18]

properties of the heme,[18] establishing the identity and spatial disposition of amino acid side chains in the heme pocket thought to participate in some major fashion in the catalytic cycle,[19] and defining the hydrogen-bonding network utilized by peroxidases in fine-tuning the reactivity of the iron center, all for a reasonably large enzyme (42 kDa) and solely in solution. This NMR data has been interpreted on the basis of the proposed sequence homology to CcP,[20] as recently supported by computer modeling of the heme cavity of HRP.[21]

In the first of three papers we have demonstrated[18] that a combination of all four methods can be utilized to locate and assign each and every one of the 22 nonequivalent sets of protons of the heme group and that their assignment provides key information on the location of the magnetic axes and the signs of the magnetic anisotropies (Figures 1 and 2). In the second of these reports,[19] we utilized the predicted dipolar field of the heme iron in conjunction with NOE measurements among amino acid side chain protons, and between such protons and previously assigned heme signals, to identify the key residues in controlling peroxidase activity, the proximal His-170, and the distal residues Arg-38 and His-42 and to show that the heme pocket is highly homologous to that of CcP,[7] as proposed earlier based on computer modeling[21] (Figures 1 and 2). The location of the substrate binding site was also established. Our third and present paper deals with characterizing the hydrogen-bonding networks that modulate the reactivity of these residues and contribute to the binding of ligands.

This present paper therefore focuses primarily on the NMR spectral properties of labile protons in or near the heme pocket as detected in H_2O rather than ^2H_2O solutions of HRPCN. Their proximity to the iron in the heme pocket can be established by the observation of either significant hyperfine shifts and/or paramagnetic relaxation effects from the iron.[22,23] While very few such resonances can be resolved or assigned in a paramagnetic protein of this size, we show that those signals that we identify allow us to provide some answers to several of the outstanding questions concerning the heme cavity of HRPCN. Moreover, the success of the methodology in characterizing HRPCN in substantial detail provides the incentive for applying our developed methodology to wider classes of the less well characterized and larger heme enzymes, such as chloroperoxidase,[25] lactoperoxidase,[26,27] and myeloperoxidase.[28]

The questions we pose here are as follows. (1) Where does the proton bind that invariably accompanies anion binding to peroxidases?[5] (2) What is the state of protonation of the distal His-42 and the nature of the interaction between this distal residue and the bound ligand? (3) What is the state of protonation of the proximal His-170 ring?[14] The methodologies utilized, saturation-transfer spectroscopy, NOEs, differential relaxation, and direction of predicted dipolar shifts, have been covered in detail earlier[18,19] and are extended here to work in H_2O solution.

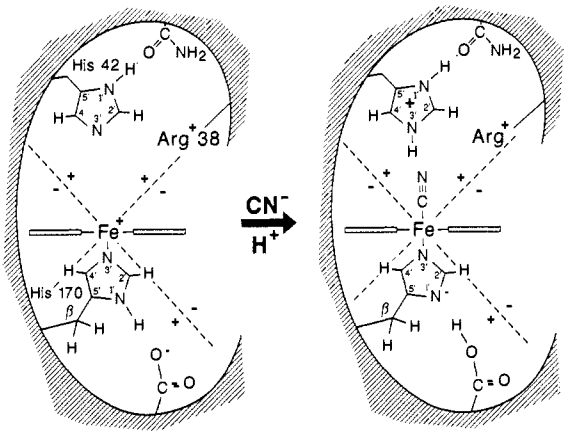

Figure 2. Schematic representation of the structure of the active site in resting-state HRP and cyanide-ligated HRPCN. In the resting state (left), the N_1H of both proximal (His-170) and distal (His-42) histidines are involved in hydrogen bonding. The proton taken up upon cyanide binding goes to the N_3 atom of His-42 and hydrogen bonds to the cyanide ligand (right). Also, the in-plane movement of the iron pulls the proximal histidine toward the heme thereby leaving the N_1 proton with the amino acid acceptor (see text). The proximity of Arg-38 to the iron in the distal side is also shown. The dashed lines define the cone at the magic angle, and the direction of the axial dipolar shift is shown, with downfield shifts as positive and upfield shifts as negative.[18,19]

Experimental Section

Sample Preparation. Horseradish peroxidase (HRP), type VI, was purchased from Sigma as a lyophilized, salt-free powder; the protein is predominantly isozyme C. The detailed purification, activity assay, and electrophoretic characterization of the protein type used in this study has already been published.[11] In practice, none of the NMR observable properties differed between our purified protein and the Sigma type VI, hence the latter was used directly without further purification. Solutions for proton NMR studies were 3 mM in protein in 90% H_2O/10% ^2H_2O. The solution pH, adjusted with 0.2 M HCl or 0.2 M NaOH in 90% H_2O/10% ^2H_2O, was measured with a Beckman Model 3550 pH meter equipped with an Ingold microcombination electrode; pH values are not corrected for the isotope effect. Excess solid KCN was added to the protein to generate solutions of HRPCN. For the experiments utilizing a mixture of HRP/HRPCN as described below, the appropriate fractional equivalent of cyanide was added in 90% H_2O/10% ^2H_2O. Typically a mixture of HRP/HRPCN in the ratio 35:65 was used for saturation transfer experiments.

Spin–Lattice Relaxation Time. Nonselective T_1s were determined by a variation of the standard inversion–recovery sequence to include a composite 180° pulse.[29] The H_2O signal in the 90% H_2O sample was saturated off-acquisition with the decoupler. In the presence of exchange with solvent, the measured effective T_1 contains contributions from intrinsic T_1 and exchange rate.[30] The effective T_1 was computed by a nonlinear least-squares fit to the equation

$$(I_\infty - I_\tau)/2I_\infty = A \exp(-\tau/T_{1\text{eff}}) \quad (1)$$

where I_τ and I_∞ are the intensities of the resonance at τ and $>5T_1$ after the 180° pulse, and τ is the delay, in milliseconds, between the 180° and 90° pulses. The intrinsic T_1 was extracted from the effective T_1 using the known relation

$$T_1^{-1} = T_{1\text{eff}}^{-1} F \quad (2)$$

where F is the saturation factor and can be obtained from the saturation transfer experiment described below. The necessarily dipolar paramag-

(25) Goff, H. M.; Gonzalez-Vergara, E.; Bird, M. R. *Biochemistry* **1985**, *24*, 1007–1013.
(26) Goff, H. M.; Gonzalez-Vergara, E.; Ales, D. C. *Biochem. Biophys. Res. Commun.* **1985**, *133*, 794–799.
(27) Shiro, Y.; Morishima, I. *Biochemistry* **1986**, *25*, 5844–5849.
(28) Harrison, J. E.; Pabalan, S.; Schultz, J. *Biochim. Biophys. Acta* **1978**, *536*, 341–349.
(29) Freeman, R.; Kempsell, S. P.; Levitt, M. H. *J. Magn. Reson.* **1976**, *38*, 453.
(30) Cutnell, J. D.; La Mar, G. N.; Kong, S. B. *J. Am. Chem. Soc.* **1981**, *103*, 3567–3572.

netic relaxation that determines T_1s for a noncoordinated residue[30,31] dictates that for two nonequivalent protons i and j:

$$R(\text{Fe–i})/R(\text{Fe–j}) = (T_{1i}/T_{1j})^{1/6} \quad (3)$$

where R(Fe–i), R(Fe–j) are their distance to the paramagnetic center. The distance of a proton from the iron is calculated by using 3-CH_3 (R(Fe–CH_3) = 6.1 Å) as reference in the above equation.

Saturation Transfer Experiment. The interconversion between HRP and HRPCN in a sample containing both HRP and HRPCN can lead to magnetization transfer between resonances in the two states due to CN^- exchange.[18,19] In a sample of pure HRPCN in 90% H_2O, saturation of the solvent signal may also lead to saturation transfer to exchangeable proton peaks.[30] In both cases, the saturation factor F is defined as

$$F = I/I_0. \quad (4)$$

where I and I_0 are the intensities of the detected signal with and without saturation of the desired peak in HRP or the solvent signal in HRPCN.

Saturation transfer experiments between HRP and HRPCN were conducted on a Nicolet NT-360 FT NMR spectrometer operating at 360.065 MHz in the quadrature mode and using 16 384 data points collected over a 80-kHz bandwidth. The data were collected by using the WEFT (water-eliminated Fourier transform) method[32] in a fashion similar to that described for the NOE experiment described below, with the preparation pulse time of 225 ms. A total of 512 scans were acquired sequentially into each interleaved data set, and the total number of scans per file was (15–20) × 10^3. The method for obtaining saturation transfer from bulk water to labile proton peaks in 90% H_2O solution of HRPCN is described elsewhere.[30]

Nuclear Overhauser Effect. The NOE,[33] $\eta_{i\to j}$, is defined as

$$\eta_{i\to j} = (I_j - I_j^0)/I_i^0 \quad (5)$$

where I_j and I_j^0 are intensities of the signal from the detected proton H_j with and without saturating the resonance of the spin H_i. The steady-state NOE for an isolated two spin system is given by

$$\eta_{i\to j} = \sigma_{ij}T_{1j} \quad (6)$$

where T_{1j} is the selective spin–lattice relaxation time of H_j, and σ_{ij} is the cross-relaxation between H_i and H_j. Since $\sigma_{ij} \propto [1/r(\text{i–j})]^6$ and $T_{1j} \propto [R(\text{Fe–j}]^6$ (eq 3), where r is the distance of the vector defining H_i and H_j and R_j is the distance of the proton H_j from the iron, eq 6 can be rewritten as

$$\eta_{i\to j} \propto [R(\text{Fe–j})/r(\text{i–j})]^6 \quad (7)$$

Under the steady-state conditions (irradiation times > 100 ms), spin diffusion[18,34] becomes important and obscures the primary NOEs. It is found that an irradiation time of 30 ms is close to the steady-state condition (eq 6) without significant spin-diffusion.[18]

Proton NOE measurements were performed on a Nicolet NM-500 FT NMR spectrometer operating at 500.027 MHz in the quadrature mode, with 16 384 data points collected in double precision over a 35-kHz bandwidth. The NOE experiments were performed according to

$$(A[t_1 - t_{on} - P - \text{Acq}]_nB[t_1 - t_{off} - P - \text{Acq}]_n)_m$$

where A and B designate two different data files, t_1 is a preparation time to allow the relaxation of the resonances (400 ms), t_{on} is the time during which the resonance is kept saturated (30 ms), and t_{off} is an equal time (30 ms) during which the decoupler is set off-resonance. P, the observe pulse, was either a Redfield 2–1–4–1–2 excitation[35] or a 1–3–3–1 pulse train.[36] In both cases some attenuation of the transmitter power was applied to obtain a $\pi/2$ pulse at the carrier (2–1–4–1–2) or to obtain a reliable 1 pulse in the 1–3–3–1 train; n was set to 96, and the total number of scans in each file (n*m) was (6–7.5) × 10^3. The NOE difference spectrum was obtained by subtracting B from A. Use of 1–3–3–1 or Redfield 2–1–4–1–2 pulse sequence, however, gives a narrow window of excitation and it is not possible to excite all the resonances evenly in the spectrum window (–10 to 30 ppm) needed for HRPCN. This leads to the situation that more than one experiment is necessary to obtain the NOE connectivities from a single peak.

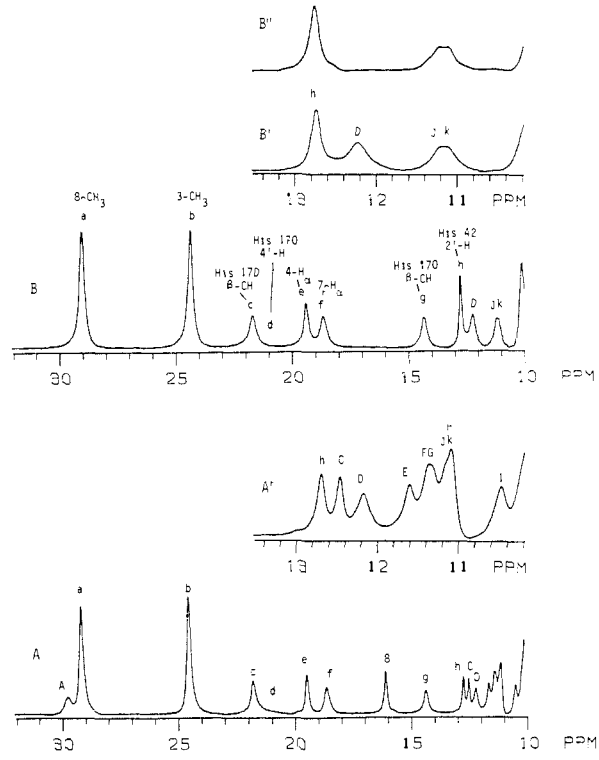

Figure 3. The hyperfine-shifted portions of the 500-MHz ^1H NMR spectrum of 3 mM HRPCN dissolved in 90% H_2O/10% ^2H_2O (A) and in 99.9% ^2H_2O (B) at 45 °C, pH 6.25. The spectrum in 90% H_2O/10% ^2H_2O was collected with use of a Redfield 21412 pulse sequence[35] with the window optimized in the region 10–30 ppm. The expanded portions of the spectra in the region 10–13 ppm are shown in inserts A′ and B′, respectively. The nonlabile proton peaks are labeled in lower-case letters, while the labile proton peaks are labeled with upper-case letters. The previous assignments of nonlabile protons is given in the spectrum in ^2H_2O. Trace B″ illustrates a portion of the spectrum obtained by using the protein reconstituted with apo-HRP equilibrated in ^2H_2O (see text). Note that peak D is missing in trace B″, indicating that it arises from a labile proton.

In some cases, ^1H NMR spectra of HRPCN in 90% H_2O/10% ^2H_2O were recorded by use of the WEFT method[32] according to

$$(A[t_1 - I - t_{on} - D_1 - P - \text{Acq}]_nB[t_1 - I - t_{off} - D_1 - P - \text{Acq}]_n)_m$$

where I represents magnetization inversion with a composite pulse 90–240–90 and D_1 is the delay time. The rest of the symbols have the same meaning as in the pulse sequence for the NOE experiment. The delay time D_1 was adjusted so that the solvent signal has minimum magnetization in the z axis. The NOE and saturation transfer measurements on slowly exchanging signals in 90% H_2O/10% ^2H_2O were carried out by using the WEFT method.

Isotope Dilution. In cases where an NOE occurs in the unresolved diamagnetic envelope, it necessary to determine if the signal is due to an exchangeable or a nonexchangeable proton. This can be achieved unambiguously by comparing the 0–10 ppm region of the NOE difference spectrum in 90% H_2O/10% ^2H_2O with that in 45% H_2O/55% ^2H_2O. Thus, irrespective of the nature of the signal being irradiated, labile or nonlabile, the same magnitude for an NOE calculated with eq 5 in both 45% H_2O and 90% H_2O is indicative of a NOE to a nonlabile peak, while a half-reduced magnitude of the NOE in 45% H_2O compared to that in 90% H_2O infers that the signal originates from an exchangeable proton.

In all of the above ^1H NMR measurements, the signal-to-noise ratio was improved by exponential apodization, which introduced 10–30 Hz line broadening. Peak shifts were referenced to the residual water signal, which in turn was calibrated against internal 2,2-dimethyl-2-silapentane-5-sulfonate, DSS. Chemical shifts are reported in parts per million, ppm, with downfield shifts taken as positive.

Results

The low-field resolved portion of the 500-MHz ^1H NMR spectrum of HRPCN dissolved in 90% ^1H_2O/10% ^2H_2O and in

(31) Swift, T. J. In *NMR of Paramagnetic Molecules*; La Mar, G. N., Horrocks, W. D., Jr., Holm, R. H., Eds.; Academic: New York, 1973; pp 53–83.
(32) Patt, S. L.; Sykes, B. D. *J. Chem. Phys.* **1982**, *56*, 3182–3184.
(33) Noggle, J. H.; Shirmer, R. E. *The Nuclear Overhauser Effect*; Academic: New York, 1971.
(34) Kalk, A.; Berendsen, J. J. C. *J. Magn. Reson.* **1976**, *24*, 343–366.
(35) Redfield, A. G.; Kunz, S. D.; Ralph, E. K. *J. Magn. Reson.* **1975**, *19*, 114–117.
(36) Hore, P. J. *J. Magn. Reson.* **1983**, *55*, 283–300.

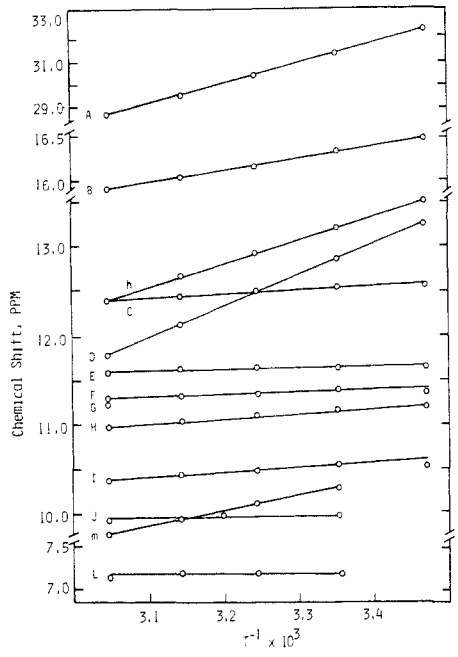

Figure 4. Curie plots of chemical shifts versus reciprocal temperature of the exchangeable and newly assigned nonlabile resonances in HRPCN at pH 6.3. The extrapolated diamagnetic intercept at $T^{-1} = 0$ is given in Table I; peak labeling is the same as in Figure 3 and Table I.

100% ^2H_2O at 45 °C are illustrated in A and B of Figure 3, respectively. Previously assigned nonlabile proton signals are designated by lower case letters; the presently located labile proton peaks are identified by upper case letters. Two obvious hyperfine-shifted labile proton peaks, A and B, are readily identified; other such protons appear in the crowded region 10–13 ppm. This region for trace A and B is presented on an expanded scale in A′ and B′ of Figure 3, respectively. Six additional exchangeable proton peaks, C and E–I, are identified (labile proton peak D was earlier considered nonlabile; see below), with C, E, and I clearly resolved, F and G overlapping each other, and H superimposed on the two nonlabile single-proton peaks previously labeled j, k.[19] Comparison of either normal or Redfield-type traces in ^1H_2O and ^2H_2O, in conjunction with variable-temperature studies, which provide differential resolution through the crowded 10–13 ppm window, establish that each of the peaks A–I originates from a single proton. The temperature dependences of the chemical shifts, presented as a Curie plot, are found in Figure 4. The temperature was selected for various experiments to provide optimal resolution and line widths.

One unusual labile proton peak is identified in the HRPCN trace obtained from a sample prepared from hemin and apo-HRP that had been soaked in ^2H_2O for several hours, as illustrated in the expansion at 45 °C in B″ of Figure 3. The peak D, previously thought to be a nonexchangeable peak because of the persistence in ^2H_2O solution even after several months,[13,19] arises from a very slowly exchanging proton in the holoprotein. The upfield portion of the resolved ^1H NMR trace fails to yield any sign of exchangeable peaks at higher fields than −2 ppm (not shown). The chemical shifts of the observed exchangeable peaks at 55 °C, as well as the apparent intercepts from Curie plots at $T^{-1} = 0$, are given in Table I. It is noted in Figure 4 and Table I that labile proton peaks A, B, and D exhibit significant hyperfine shifts (as does the nonlabile His-42 4′-H, peak m), as evidenced by the slope of the plot. The remaining labile proton peaks, C and E–L, exhibit only very weak or no detectable temperature dependence, suggestive of a primarily diamagnetic environment distant from the heme pocket.

Spin–Lattice Relaxation Times. The effective spin–lattice relaxation times were determined by the inversion–recovery method for 3-CH_3 and the resolved exchangeable signals A and B in 90% H_2O/10% ^2H_2O at 360 MHz, 35 °C. The H_2O signal was saturated off-acquisition with the decoupler. Both the signals A and B show saturation transfer from H_2O, and the intrinsic T_1 values were calculated taking into account the saturation factor[30,37] and are found to be 20 and 240 ms for the signals A and B, respectively. The heme 3-CH_3 signal, with negligible diamagnetic contribution to its T_1 relaxation, serves as reference proton (H_j) in eq 3, with T_1(3-CH_3) = 61 ms at 35 °C and r(3-CH_3–Fe) ~ 6.1 Å. Such analysis yields iron–proton distances of 5.0 and ~7.5 Å, respectively, for the signals A and B.

Table I. Chemical Shifts and Assignments of Amino Acid Protons in HRPCN at pH 7.0, 55 °C[a]

peak designation	assignment[b]	shift, ppm	intercept at $T^{-1} = 0$, ppm[c]
A	His-42 3′-H	28.72	0.5
B	His-42 1′-H	15.91	11.5
h	His-42 2′-H	12.45	3.6
m	His-42 4′-H	9.76	4.5
D	His-170 peptide NH	11.81	1.0
J	His-170 ring NH	9.93	9.9
K	Tyr-185 ring OH (?)	7.27	
C	*d*	12.45	11.1
E	*d*	11.55	11.0
F	*d*	11.29	10.3
G	*d*	11.21	10.2
H	*d*	10.98	8.4
I	*d*	10.35	8.7
L	*d*	7.13	7.1

[a] Chemical shifts in ppm are referenced to DSS through the water signal; uncertainty in shifts ± 0.02 ppm; the remaining assignments of nonexchangeable heme and amino acid resonances in the heme pocket of HRPCN are given in ref 18 and 19. [b] Tentative assignments are marked by (?). [c] From extrapolation of straight lines in Figure 4. [d] No paramagnetic influence noted, assignments not pursued.

Distal Residues. There are two distal residues whose side chains place labile protons close to the heme iron based on the established homology to *Cc*P,[7,19-21] His-42, and Arg-38 (Figure 2). The former group possesses one or two labile ring protons, depending on the state of protonation of the imidazole ring, while the latter group possesses five labile protons on the guanidyl group, of which four exist as two pair of close neighbors (1.65 Å); members of different pairs are separated by only 2.3 Å.

Figure 5A illustrates the 500-MHz Redfield ^1H NMR spectrum of HRPCN in 90% H_2O/10% ^2H_2O at 45 °C (where h and C are resolved), with the spectral window optimized for the region 9.5–30 ppm. Saturation of the assigned His-42 proton h (attributed to 2′-H rather than 4′-H based on its shift[19]), yields detectable NOEs only to the two labile proton peaks A and B (Figure 5B). Saturation of peak A yields the expected reciprocal NOE to peak h, as well as one to a peak at 9.8 ppm, which we designated m (Figure 5C). The fact that the magnitude of the NOE to m is unaltered upon isotope dilution (not shown) dictates that peak m arises from a nonexchangeable proton. Irradiation of labile proton peak B yields an NOE to peak h (Figure 5D) of the same magnitude (~8%) as observed when peak A was saturated (Figure 5C). This requires that proton h (His-42 2′-H) is equidistant from protons A and B. The absence of detectable NOEs to other labile proton peaks upon saturating either peak A or B is noted.

In order to observe NOE connectivities within the intense diamagnetic envelope, saturations of peaks A, B, and h are repeated at 45 °C with a spectral window optimized for the low-field side of the solvent resonance to 7 ppm (Figure 6A). Irradiation of peak B fails to yield any NOEs to any other labile proton, exhibiting only the reciprocal NOE to h (Figure 6B). Saturation of peak A at 28.7 ppm yields the trace shown in Figure 6C. Since the spectral window in Figure 6 is symmetric about a point midway between peaks h and m, the observation of similar NOEs to h and m upon saturating A (Figure 6C) suggests that nonlabile proton h and m are at comparable distances from labile proton A (if the relaxation properties of h and m are the same). The line width for peak m (determined in the NOE difference trace in Figure

(37) De Ropp, J. S. Ph.D. Thesis, University of California, Davis, 1981.

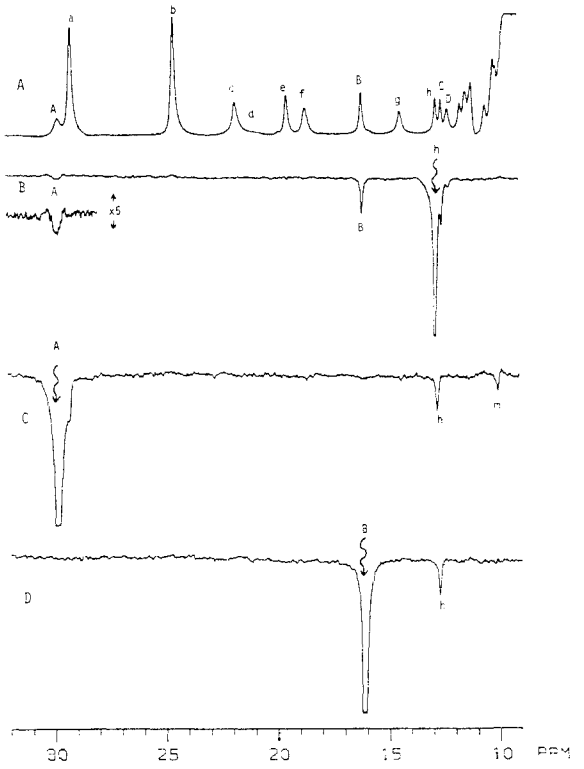

Figure 5. The hyperfine-shifted portions of the 500-MHz ^1H NMR spectrum of (A) 3 mM HRPCN in 90% H_2O/10% ^2H_2O at 45 °C, pH 6.25. The spectrum was collected with use of a Redfield 21412 pulse sequence[35] with the spectral window optimized in the region 10–30 ppm. Peak labeling is the same as in trace A of Figure 3. B–D are the NOE difference spectra generated by subtracting the reference spectrum with decoupler off-resonance from a similar spectrum of the same sample in which the desired resonance was saturated. In each of the difference spectra a downward arrow indicates the peak being saturated. (B) Saturation of peak h (2′-H of His-42) showing NOEs to peaks A and B. (C) Saturation of peak A showing the reciprocal NOE to peak h and an NOE to peak m. (D) Saturate peak B; note the reciprocal NOE to peak h. Also note the very similar intensity of peak h upon saturating peaks A and B (traces C and D).

6C) is comparable to that of h, and narrower for both h and m than expected for any but the relatively isolated 2′-H or 4′-H of an imidazole or indole side chain (Figure 2). These similar line widths support similar relaxation properties of h and m.

The absence of dipolar connectivities between the labile protons A and B and any other labile proton with shift to the low field of the water resonance dictates that these are relatively isolated from other labile protons and hence makes them very unlikely candidates for the Arg-38 side chain. The absence of any dipolar connectivities of nonlabile proton peak h to other nonlabile protons has already established[19] that it arises from the relatively isolated 2′-H or 4′-H of the distal His-42. The only other amino acid with such an isolated proton, Trp (the 2′-H), does not occur near the heme in HRP.[38] The presence of strong dipolar connectivities from peak h to the two hyperfine shifted labile protons, A and B, makes them strong candidates for the labile proton 1′-H and 3′-H of a protonated imidazole side chain (Figure 2), and confirms that h is due to 2′-H rather than 4′-H of His-42. This assignment is completely consistent with the observation that $\eta_{A\rightarrow h} = \eta_{B\rightarrow h}$, as required by the geometry of the imidazolinium side chain.

The similar line widths of peaks h and m (as determined solely in the difference spectrum in Figures 5C, 6C) support similar relaxation properties and suggest comparable distance between A and h and A and m. Moreover, the small line width for peak m (as was previously assigned for peak h) in such a large protein is indicative of the relatively isolated His 2′-H and 4′-H. Thus

(38) Ohlsson, P.-I.; Horie, T.; Vanderkooi, J. M.; Paul, K.-G. *Acta Chem. Scand., Ser. B* **1986**, *B40*, 257–261.

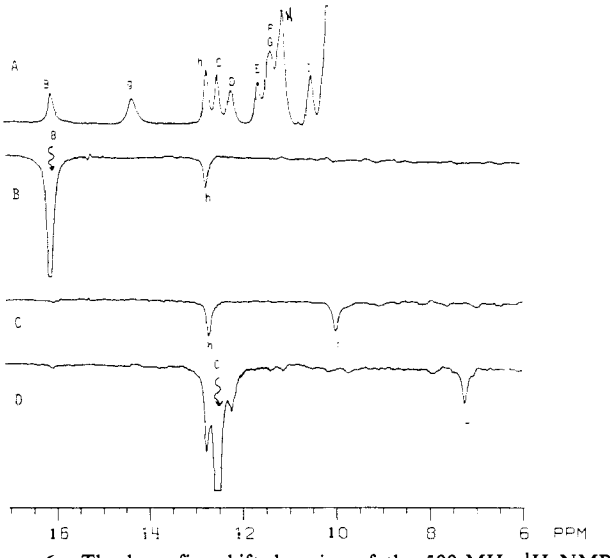

Figure 6. The hyperfine-shifted region of the 500-MHz ^1H NMR spectrum of (A) 3 mM HRPCN in 90% H_2O/10% ^2H_2O at 45 °C, pH 6.25. The spectrum was collected with use of a Redfield 21412 pulse sequence[35] with the spectral window optimized in the region 6–17 ppm. The well-resolved signals are labeled. The NOE difference spectra B–D are generated as described in Figure 5. The downward arrow shows the peak being saturated. (B) Saturate peak B; note the sole NOE to peak h. (C) Saturate peak A (the peak is off scale on left and not excited by the observation pulse) showing NOEs to peaks h and m; note that the intensities of peaks h and m are similar, indicating that they are at comparable distances from the proton responsible for the peak A (see text). (D) Saturate peak C; note NOE to peak L. Dilution with ^2H_2O suggests peak L is also from an exchangeable proton.

we assign nonlabile proton m to His-42 4′-H. This serves to confirm A as 3′-H and h as 2′-H and supports B as originating from 1′-H. Based on the established homologous stereochemistry of the heme pockets in HRP[21] and *Cc*P,[7] the X-ray structure of the latter predicts[7] that the distal His 3′-H is ~5.0 Å from the iron, while 1′-H is ~7.5 Å from the iron. These distances are the same as the values of 5.0 and 7.5 Å determined above from differential iron-induced relaxation. The very large downfield (necessarily) dipolar shift for peak A is also consistent with its location close to the iron and along the pseudo-fourfold axis, for which the known magnetic properties of the iron predict such dipolar shifts[18,19] (Figure 2). Thus the peaks B, h, A, and m arise from the His-42 ring proton 1′-H, 2′-H, 3′-H, and 4′-H (Figure 2), with stereochemistry very similar to that of the distal His-52 in *Cc*P.[7]

No NOEs to labile protons could be detected when the known Arg-38 side chain methylene proton peaks[19] at −4.8 and −5.2 were saturated (not shown). However, these two protons have been assigned[19] to the β-CH and δ-CH, respectively, which are not expected to be close to a labile proton. The other identified Arg-38 side chain nonlabile protons resonate much too close to the diamagnetic envelope to allow detection of useful NOE difference spectra due to strong off-resonance saturation of the diamagnetic envelope and the strong solvent signal. However, saturation of any of the remaining unassigned labile protons, C and E–I (see below), failed to yield any NOEs at the known resonance position of the Arg-38 side chain nonlabile peaks, making it very unlikely that any of them originated from the terminal guanidyl group.

Upon inspection of the ^1H NMR spectra of HRPCN in pure ^2H_2O and 90% H_2O, we find that, besides the absence of the exchangeable protons A–I in the deuteriated solvent, there *appears to be a small solvent isotope effect on the shifts of the heme resonances*. For example, the 8-CH_3 resonance yields two resolvable components in various $^1H_2O/^2H_2O$ solvent mixtures with relative intensities that are the same as the solvent isotope composition (Figure 7A–C). The left and right components correspond to the state containing the proton and the deuteron, respectively (Figure 7B). When the pH is raised for the 1:1 $H_2O/^2H_2O$ solution, the partially resolved pair of 8-CH_3 peaks

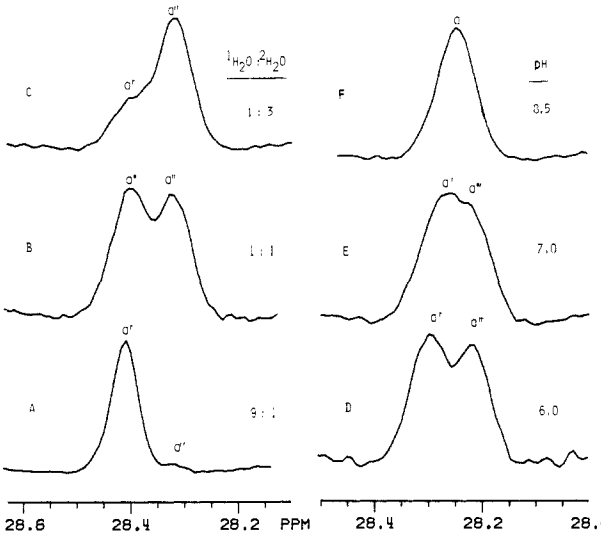

Figure 7. Effect of solvent composition (traces A–C) and pH (traces D–F) on the heme 8-CH_3 resonance region of the 500-MHz ^1H NMR spectrum of 2 mM HRPCN at 55 °C; (A) 90% H_2O/10% ^2H_2O, pH 5.0; (B) 50% H_2O/50% ^2H_2O, pH 5.0; (C) 25% H_2O/75% ^2H_2O, pH 5.0. Spectra of 2 mM HRPCN in 50% H_2O/50% ^2H_2O at 55 °C, pH 6.0 (D), 7.0 (E), and 8.5 (F). The H_2O and ^2H_2O components of the 8-CH_3 resonance are labeled as a′ and a″, respectively, while the labeling a represents the collapsed signal at high pH. All the spectra were resolution-enhanced by multiplying the free-induction decay with a sine-bell function prior to Fourier transformation.

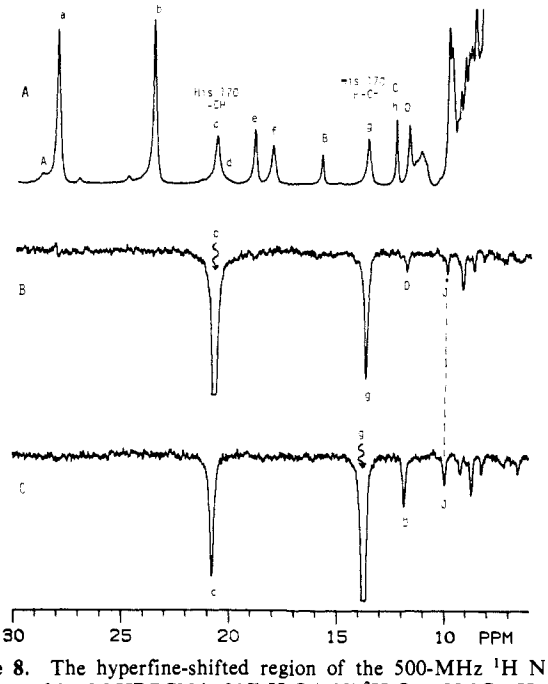

Figure 8. The hyperfine-shifted region of the 500-MHz ^1H NMR spectrum of 3 mM HRPCN in 90% H_2O/10% ^2H_2O at 55 °C, pH 6.25. The peaks are labeled as in trace A of Figure 3. Spectra were collected by the WEFT method.[32] The H_2O signal was suppressed by using a delay time of 450 ms in between the 180° pulse and the observe pulse. B and C are the NOE difference spectra generated as described in Figure 5 upon saturating the known[19] His-170 H_β peaks c and g, respectively; note the NOEs to the labile proton peaks D and J.

dynamically collapses to yield a single peak (Figure 7D–F), in spite of a chemical-shift difference between H_2O and ^2H_2O. It has been observed that peaks A and B are clearly resolved at pH 5, but as the pH is raised, while peak B is essentially unaffected, peak A broadens and loses its intensity at alkaline pH, indicating exchange with bulk solvent.[37]

Proximal Histidine. The previous NOE studies of HRPCN in ^2H_2O have shown that peak D (previously labeled[18] as non-exchangeable proton i) yields a strong NOE from one of the

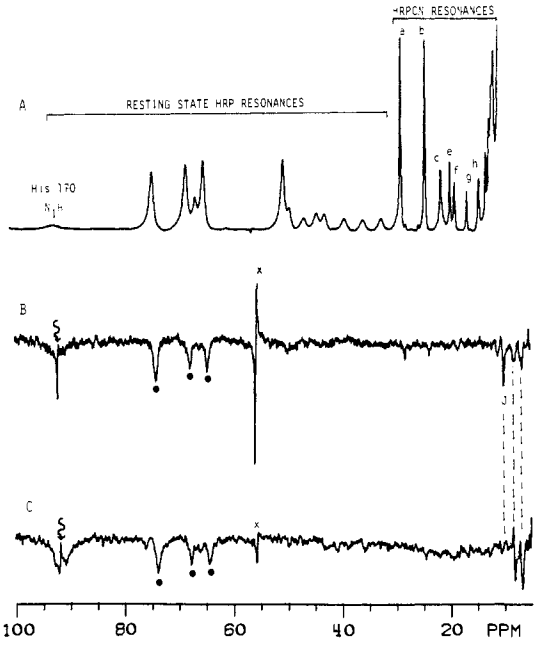

Figure 9. The hyperfine-shifted portion of the 360-MHz ^1H NMR spectrum of a mixture of HRP/HRPCN in the ratio 40:60 in 90% H_2O/10% ^2H_2O at 55 °C, pH 6.3. The spectra were collected by using the WEFT method.[32] The difference spectra B and C are generated as described in Figure 5. A filled circle denotes the off-resonance perturbation of the decoupler power. (B) Saturation of the His-170 N_1H at 92 ppm in resting-state HRP showing saturation transfer to its counterpart (peak J) in HRPCN. (C) Difference spectrum obtained by employing HRP alone (without CN^-) under identical conditions; note the disappearance of peak J.

proximal His-170 β-CH's, as confirmed in ^1H_2O solution in Figure 8. With the present knowledge that this peak arises from an exchangeable proton, we can definitely assign it to the peptide NH of the same residue, for which the *Cc*P structure predicts[7] close distances (2.5 Å) to one of the β-CH's. Thus the very similar stereochemistry of the axial His in *Cc*P and HRP is further confirmed. The unusually slow exchange behavior of this peptide proton with bulk solvent in the holoprotein is further testimony to the extraordinary dynamic stability of the heme pocket of HRP.[37,39]

The ^1H NMR spectrum of partially cyanide ligated HRP in 90% H_2O is shown in Figure 9A. The high-spin HRP signals[11] are in the region 40–100 ppm, while the low-spin HRPCN peaks occur exclusively upfield of 40 ppm. Known assignments in both HRP states are given.[11,13,17,39,40] Irradiation of the previously assigned[39] His-170 ring N_1H labile proton peak at 92 ppm in HRP in the presence of HRPCN shows saturation transfer to peak J at 9.9 ppm (trace B). When this signal at 92 ppm is saturated in a HRP sample without CN^-, this peak J at 9.9 ppm is not observed (trace C). Since the assignment of His-170 N_1H in resting state HRP is unambiguous,[39] the saturation transfer to its counterpart *in HRPCN identifies the peak J as arising from this same labile proton in whatever state it exists in HRPCN.*

Having identified the proton signal in HRPCN originating from that proton that was the proximal His-170 ring NH in HRP, the next step is to establish its location and environment in the vicinity of the proximal His. The occurrence of peak J under the diamagnetic envelope precludes direct determination of its T_1 value. Qualitative consideration of the line width (as obtained from the saturation transfer difference trace in Figure 9B) relative to that of a heme methyl, however, is illuminating. We find the line width of J to be essentially the same as that of the heme methyl signal 3-CH_3 (~70 Hz) in HRPCN. In low-spin ferric cyanide com-

(39) La Mar, G. N.; de Ropp, J. S. *Biochem. Biophys. Res. Commun.* **1979**, *90*, 36–41.
(40) Thanabal, V.; de Ropp, J. S.; La Mar, G. N., manuscript in preparation.

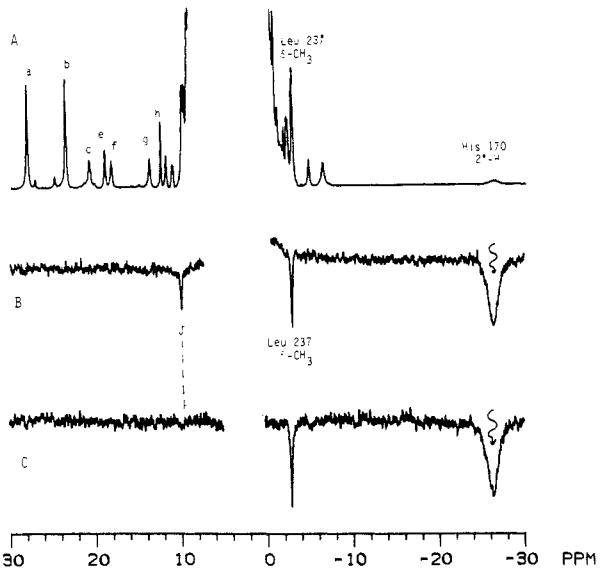

Figure 10. The hyperfine-shifted protion of the 500-MHz ^1H NMR spectrum of (A) 3 mM HRPCN freshly dissolved in 99.9% ^2H_2O at 55 °C, pH 7.0. Previously assigned[19] His-170 2′-H and Leu 237 δ-CH_3 signals are labeled. B and C are the NOE difference spectra obtained as described in Figure 5 upon saturating the His-170 2′-H peak. (B) The NOE difference spectrum obtained within 2 h after dissolving HRPCN in fresh ^2H_2O; note the NOE to peak J, in addition to the previously observed[19] NOE to Leu-237 δ-CH_3 signal. (C) The NOE difference spectrum obtained with the same sample as in B after 24 h at 55 °C. Now, note the disappearance of the peak J, indicating the labile nature of this proton.

plexes of myoglobin,[30,41-43] and legume hemoglobin,[44] the proximal His ring NH was consistently found to exhibit 20–30% greater line width than the heme methyl, which is consistent with the larger paramagnetic contribution to the ring NH line width (5.1 Å from the iron) relative to that of the heme methyl (6.1 Å from the iron). Since the axial His ring NH is narrower, as compared to a heme methyl, in HRPCN than metMbCN,[30,41-43] *we conclude that the ring labile proton J is further from the iron in HRPCN than metMbCN.* In the latter protein, this proton is unquestionably associated solely with the neutral imidazole ring.[30,43] A quantitative distance estimate for R(Fe–J) via an equation similar to eq 3 but using line width is not valid because of the very large diamagnetic contributions to the line width.

In order to assess how close to the original site on the His-170 ring the labile proton J now finds itself, we turn to NOEs from the other known His-170 nonlabile proton signals, the ring 2′-H[45] at −26.3 ppm, and the pair of β-CH's[19] at 20.8 and 13.8 ppm. Saturation of His-170 β-CH signals in a 90% H_2O solution of pure HRPCN yields NOEs of 7–10% (Figure 8B,C) to a peak at precisely the same resonance position, 9.9 ppm, as peak J; thus, we must assume the NOEs in Figure 8B and C are to peak J. Thus J is still close to the His-170 β-CH. The X-ray structure of the homologous CcP[7] indicates a β-CH–N_1H distance of 2.8 Å. The observed NOE suggests that this separation could not have increased to much over 3 Å. The X-ray data on CcP,[7] moreover, predict a short 2′-H–1′-H distance of 2.6 Å. Saturation of the broad His-170 2′-H resonance[44] at −26.3 ppm in a sample of HRPCN freshly dissolved in ^2H_2O yields an NOE at 9.9 ppm (Figure 10B) whose origin must be peak J, inasmuch as we have conclusively demonstrated that the His-170 N_1H proton exchanges slowly (half-life ~ 2 h at 55 °C) in both the resting state[39] and cyanide complexes.[46] The identification with the His-170 N_1H

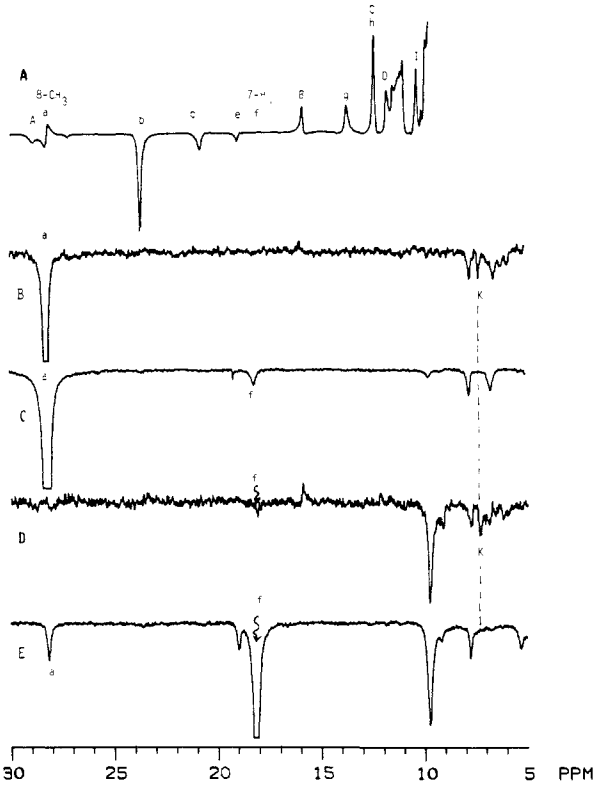

Figure 11. The hyperfine-shifted portion of the 500-MHz ^1H NMR spectrum of (A) 3 mM HRPCN in 90% H_2O/10% ^2H_2O at 55 °C, pH 6.25. The spectrum was collected by using the $1\bar{3}3\bar{1}$ pulse sequence,[36] and the spectral window was optimized for the region 5–15 ppm. The downfield 15–25 ppm region is the second excitation window of the pulse sequence, and the signals in this region have opposite phase according to the phase modulation of the $1\bar{3}3\bar{1}$ pulse train.[36] Peaks a (8-CH_3) and f (7-Hα) fall on the crossover points of the excitation windows and hence these resonances are not excited. B–E are the NOE difference spectra generated as described in Figure 5. B and D are obtained with the condition as in A and irradiating peaks a (8-CH_3) and f (7-Hα), respectively. Since peak f is not excited in the reference spectrum (A), it is missing in the difference trace (D). Note that both 8-CH_3 and 7-Hα show NOEs to peak K. Traces C and E are the conventional NOE difference spectra obtained by using HRPCN in 99.9% ^2H_2O upon irradiating peaks a and f, respectively. The absence of peak K in traces C and E indicates that peak K originates from a labile proton.

is confirmed with the observation that the NOE from 2′-H to J in ^2H_2O disappears with time as J exchanges ^1H for ^2H (Figure 10C). Following the chemical shift of peak J via variable-temperature NOE studies reveals the absence of any significant hyperfine contribution to the shift, as illustrated on the Curie plot in Figure 4. Thus NOEs establish that J is still in the proximity of the His-170 in a manner qualitatively similar to that expected for a neutral His, while its line width indicates it is further from the iron than in a neutral imidazole complex.

Peripheral Contacts. NOE studies on resolved resonances other than those discussed above failed to reveal any dipolar connectivities to labile protons (not shown), except for substituents on pyrrole IV. Saturation of 8-CH_3 in HRPCN in H_2O (Figure 11B) and ^2H_2O (Figure 11C) reveals a single labile proton peak at 7.3 ppm, which we designate K. The X-ray structure of CcP,[7] in conjunction with computer modeling of HRP,[21] reveals the presence of two side chains with labile protons within 5 Å of 8-CH_3, Arg-183 on the distal and Tyr-185 on the proximal side of the heme. Saturation of the adjacent 7-H_α peak at 18.2 ppm also yields a NOE to K (Figure 11D and E). Since the 7-propionate α-methylene group has both protons directed toward the proximal side of the heme,[21] as found in both CcP,[7] we conclude that K arises from the side chain phenolic proton of Tyr-185.

(41) Lecomte, J. T. J.; La Mar, G. N. *Biochemistry* **1985**, *24*, 7388–7395.
(42) La Mar, G. N.; Krishnamoorthi, R. *Biophys. J.* **1983**, *44*, 177–183.
(43) Lecomte, J. T. J.; La Mar, G. N. *Eur. Biophys. J.* **1986**, *13*, 373–381.
(44) Kong, S. B.; Cutnell, J. D.; La Mar, G. N. *J. Biol. Chem.* **1983**, *258*, 3843–3849.
(45) La Mar, G. N.; de Ropp, J. S.; Chacko, V. P.; Satterlee, J. D.; Erman, J. E. *Biochim. Biophys. Acta* **1982**, *708*, 317–325.
(46) De Ropp, J. S.; Thanabal, V.; La Mar, G. N. *J. Am. Chem. Soc.* **1985**, *107*, 8268–8270.

This residue has been proposed to participate in substrate binding.[21]

Other Resolved Labile Protons. The partially resolved exchangeable proton signals E → I in the region 12–10 ppm (Figure 3) exhibit essentially temperature independent shifts (Figure 4) and hence must originate from side chains removed from the heme cavity and have not been considered further; attempts to detect interpretable NOEs from peaks E–I were not successful. Saturation of labile peak C yields a NOE to a peak designated L, as shown in Figure 6D. Isotope dilution of the solvent by ^2H_2O suggests that peak L may be exchangeable. However, since neither peak C nor L exhibits any hyperfine shift (Figure 4) and is not dipolar-coupled to any assigned proton in the heme cavity, more definitive assignment was not pursued.

Discussion

The Distal H Bonding Network. The assignment of the remaining His-42 ring protons, h, m, A, and B, demonstrates that the side chain is protonated, i.e., exists as an imidazolium rather than a neutral imidazole group. Since it has been proposed[6,7] that the resting state of HRP must possess a neutral imidazole side chain for effective catalysis, our results dictate that ligation of HRP by cyanide ion is accompanied by protonation of the distal His-42 imidazole side chain. It has long been recognized that one of the distinguishing characteristics of heme peroxidases is that they bind protonated anionic ligands,[4,5,47–49] while ferric derivatives of molecular oxygen-binding proteins such as Mb and Hb bind solely the anionic ligands such as CN^-, F^-, and N_3^-. Thus we conclude that the proton accompanying anion binding to HRP ends up on the N_3 atom of the distal histidyl imidazole.

In several cases it has been suggested that the anionic ligand is actually bound in the protonated form.[47–49] Thus certain aspects of the X-ray crystal structures of the fluoro derivative of CcP[48] have been interpreted to indicate that the bound species may be actually HF rather than F^-. In the present case, the direct binding of HCN through the nitrogen can be discounted by the fact that the ^{15}N NMR signal of the bound cyanide can be detected, and its line width is inconsistent with reflecting direct N-bonding to iron(III).[50] The ligand could bind as the protonated isocyanide, CNH, but this is not likely because the NOEs from A and B to h place them at equal distance from the 2′-H and are consistent with A associated with the His-42 ring. The distance from the iron for the proton responsible for peak A, ~5 Å as determined above from the iron-induced relaxivity, places it within van der Waals contact of the bound cyanide nitrogen, but this does not indicate whether it is interacting with the ligand.

The presence of direct interaction between the His-42 imidazolium side chain and the bound ligand can be experimentally established as follows. We have shown elsewhere[51] that the NMR spectra of low-spin ferric hemoproteins often exhibit an isotope effect on the electronic structure of the heme, as manifest in the ability to resolve separate heme methyl hyperfine shifts due solely to the differences between a proton versus a deuteron on a distal residue interacting with a bound ligand. The resolution of such heterogeneity in the electronic structure is direct proof of an important link between the heme ligand and the distal residue possessing the responsible proton. As demonstrated in Figure 7, HRPCN exhibits different chemical shifts for the 8-CH_3 (as well as other peaks) depending on solvent isotope composition. The fact that there are only two contributing peaks, and their ratio of intensity corresponds to the $^1H/^2H$ isotope composition of the bulk solvent, dictates that the *isotope effect on the heme electronic structure is due exclusively to a single proton/deuteron interchange*, as found previously in metMbCN.[51] The physical origin of the labile proton/deuteron responsible for the effect can be uniquely established by recognizing that this heterogeneity is resolved only when the labile proton/deuteron exchange lifetime with bulk water is long compared to the 8-CH_3 peak shift difference (~30 Hz). At pH 5, both peaks A and B are in slow exchange with bulk water. However, as the pH is raised, we note that the two 8-CH_3 peaks broaden and collapse, yielding a narrow, averaged resonance midway between the known shifts in pure H_2O and ^2H_2O (Figure 7D → F). The labile proton peak B is essentially unaffected by pH.[37] Peak A, on the other hand, broadens as the pH is raised until it loses all intensity, indicating rapid exchange with bulk solvent[30,37] at pH above 7.5. Therefore we can conclude that the isotope splitting of the 8-CH_3 resonance is due to interaction with proton A, which has been shown to reside on the N_3 atom of His-42. Thus, the imidazolium side chain serves as a hydrogen-bond donor to the bound CN^-. The binding of CN^- and a proton in the distal heme cavity on converting resting state HRP to HRPCN can thus be envisaged as depicted in Figure 2A → B.

The fact that HRPCN does not exhibit a pK in the pH range 3–11 is a testimony to the stability of this interaction. A "normal" imidazolium side chain should deprotonate at much lower pH if they existed outside this hydrogen-bonding network. It is likely that the often-studied but poorly understood alkaline transition in HRPCN[13,15] (with pK ~ 11) simply represents the deprotonation of A (or B). It is to be noted that the hydrogen-bonding network described here has been proposed earlier[6,7] and is precisely the arrangement that would facilitate cleavage of the O–O bond in H_2O_2 to yield the oxidized ferryl ion. The carbonyl stretching frequency of CO bound to reduced HRP and CcP has been shown sensitive to solvent isotope effects,[52,53] which must reflect hydrogen bonding to the ligand, but did not provide information on the state of protonation of the His-42 side chain or the identity of the proton interacting with the ligand.

No direct information on the state of the N_1H of His-42 (peak B) is inferred from its NMR properties, except that the slow exchange with bulk solvent suggests that it participates as a hydrogen-bond donor to some amino acid side chain. Such an interaction is detected[7] between the distal His side chain in CcP and the side chain of Asn-82, and the latter residue appears conserved in HRP.[20]

The ^1H NMR data on labile protons at this time do not provide any more direct information as to the participation of other residues, such as Arg-38, in stabilizing the bonding of ligands. It is noted that the labile protons for the side chain occupy a region of space in CcP (and by homology, likely in HRP) that places them very near the magic angle for the axial dipolar shift[18,19] (as illustrated in Figure 2), as well as near a node in the rhombic dipolar shift[18,19] (over the γ-meso position; Figure 1). Hence it is not surprising that the Arg-38 side chain labile protons are not resolved outside the intense diamagnetic envelope. Another possibility is that those protons may exchange rapidly with bulk solvent.

Proximal Histidine. The potential importance of imidazolate character for the His-170 side chain in stabilizing the highly oxidized compounds I and II has been recognized for some time.[54,55] Various spectroscopic methods[56–59] have been used to support the presence of a deprotonated histidyl imidazole, but the evidence is often indirect and can be interpreted as easily by strong

(47) Erman, J. E. *Biochemistry* **1974**, *13*, 39–44.
(48) Edwards, S. L.; Poulos, T. L.; Kraut, J. *J. Biol. Chem.* **1984**, *259*, 12984–12988.
(49) Williams, R. J. P. In *Iron in Biochemistry and Medicine*; Jacobs, A., Worwood, M., Eds.; Academic: New York, 1974; pp 183–219.
(50) Behere, D. V.; Gonzalez-Vergara, E.; Goff, H. M. *Biochim. Biophys. Acta* **1985**, *832*, 319–325.
(51) Lecomte, J. T. J.; La Mar, G. N., submitted for publication in *J. Am. Chem. Soc.*
(52) Smith, M. L.; Ohlsson, P.-I.; Paul, K. G. *FEBS Lett.* **1983**, *163*, 303–305.
(53) Satterlee, J. D.; Erman, J. E. *J. Am. Chem. Soc.* **1984**, *106*, 1139–1140.
(54) Morrison, M.; Schonbaum, G. R. *Annu. Rev. Biochem.* **1976**, *45*, 861–888.
(55) Nicholls, P. *Biochim. Biophys. Acta* **1962**, *60*, 217–226.
(56) Blumberg, W. E.; Peisach, J. In *Probes of Structure and Function Macromolecules and Membranes*; Chance, B., Bonetani, T., Mildvan, A. S., Eds.; Academic: New York, 1971; Vol. II, pp 215–229.
(57) Teraoka, J.; Kitagawa, T. *J. Biol. Chem.* **1981**, *256*, 3969–3977.
(58) Desbois, A.; Mazza, G.; Stretzkowski, F.; Lutz, M. *Biochim. Biophys. Acta* **1984**, *785*, 161–176.
(59) Mincey, T.; Traylor, T. G. *J. Am. Chem. Soc.* **1979**, *101*, 765–766.

hydrogen-bond donation by the ring labile proton N_1H. ^1H NMR is ideally suited for directly probing the state of this proton. The unambiguous identification of the ring N_1H in high-spin ferric[39] and ferrous HRP,[14] where its hyperfine shift is predominantly scalar or contact in origin, has established that *His-170 is not deprotonated in the five-coordinate forms of this enzyme.* The absence of a labile proton peak attributable to the proximal His ring NH in low-spin HRPCN with hyperfine shift anywhere near that observed in isoelectronic Mb and Hb derivatives had led us to propose[46] that deprotonation does take place in six-coordinate HRPCN. A wide array of NMR spectral characteristics directly support the imidazolate description of HRPCN. Thus model compounds have demonstrated[60] that imidazolate versus imidazole low-spin ferric complexes differ in that the former exhibit a large upfield shift for 2′-H and a large downfield bias of His β-CH's, as compared to the latter. We had already demonstrated[45] that the proximal His-170 2′-H is considerably upfield, near the position in imidazolate models,[60] and not near the resonance position found in both metMbCN[45] and model compounds with neutral imidazole.[60] The recent assignments of both the proximal His β-CH's in HRPCN[19] and metMbCN[43] again demonstrate that the former exhibit much larger downfield shifts (20.8 and 13.8 ppm for a mean of 17.3 ppm) than the latter (10.4 and 6 ppm for a mean of 8.2 ppm). The fact that peak J does not exhibit any paramagnetic contribution to its shift, as illustrated in Figure 4, in contrast to the imidazole N_1H in either models[60] or metMbCN,[30] as well as its line width, is completely consistent with the imidazolate formulation for His-170.

The saturation transfer from the His-170 ring NH in HRP to peak J in HRPCN identifies this proton in the latter system. The line width for peak J, when compared to a heme methyl, dictates that the proton is further from the iron than for a neutral imidazole and hence has moved upon forming HRPCN (i.e., R(Fe–J) has increased). The NOE connectivities of the remaining His-170 nonlabile protons to peak J, however, dictate that this movement is not far, so that the alternate positions of proton J in HRP and HRPCN are relatively close. This apparent paradox can be rationalized when recognizing that such a proton shuttle that would interconvert $ImH \leftrightarrow Im^-H^+$ could require as little as 0.5-Å movement of the H^+ in a double-potential well between the imidazole N_1 and the O of some acceptor residue, such as Asp-232 found in C*c*P. Such a motion would, in effect, interconvert N_1–H···$^-$OR → N_1^-···HOR, while keeping the H^+ highly localized. This is consistent with our observation that the very slow exchange rate of N_1H with bulk solvent in resting state HRP[39] is maintained in HRPCN.[46] This motion of 0.5 Å along the original N_1H bond direction would increase the distance of proton J from His 170 β-CH_2 and 2′-H, r(c–J), by ~0.3 Å and similarly increases the distance from the iron, R(Fe–J), from 5.0 to 5.3 Å. Since the NOE, $\eta_{i\to j} \alpha [R(\text{Fe–j})/r(\text{i–j})]^6$ (eq 7), the decrease in η expected by a 10% increase in r(i–j) is largely compensated for by the 6% increase in R(Fe–j), and rationalizes the still clearly detectable NOEs from both β-CH's and 2′-H to the transferred 1′-H in HRPCN.

^{15}N NMR hyperfine shifts of cyanide bound to ferric model heme complexes[50] have been shown to serve as potential probes of either hydrogen bonding to the bound cyanide or deprotonation of the trans imidazole. It has been noted that the cyanide ^{15}N shift difference between HRPCN and metMbCN is of a magnitude that is consistent with both deprotonation of the proximal His imidazole, as well as strong hydrogen bonding on the distal side in HRPCN. Our present NMR results provide direct evidence for both of these interactions.

Thus we conclude that ligation of HRP by CN^-, together with addition of a proton, leads not only to protonation of the His-42 ring (which then hydrogen bonds to the bound cyanide) but also to the loss of the His-170 labile ring proton to some anionic acceptor such as Asp-232 found in C*c*P.[7] The changes in both the proximal and distal side of the heme pocket accompanying ligation of cyanide are depicted schematically in Figure 2. The likely reason for the apparent large change in pK of the distal His-42 upon cyanide ligation (it is neutral in HRP[6,7] and protonated in HRPCN) is precisely the loss of the proximal His-170 ring proton and is the property of peroxidases that differentiate it, as a class, from myoglobin and hemoglobins. Thus the distal His E7 imidazole ring remains neutral in both unligated and ligated states in the functional pH range for Mb and Hb.[2]

The enzymic intermediate compounds I and II are two and one oxidizing equivalent, respectively, above resting state HRP.[5,6] The conversion of HRP-II (Fe^{IV}=O) to HRP involves addition of a proton and electron and the release of a water molecule. HRP-II, like HRPCN, is six-coordinate and low-spin and possesses one more proton than resting-state HRP. By analogy to HRPCN, we can therefore infer that this added proton in HRP-II should be on the distal His-42 ring to yield an imidazolium side chain that can be expected to hydrogen bond strongly to the axial oxygen atom. This is in accord with resonance Raman studies that find a strong solvent isotope effect on the Fe=O stretching frequency.[61]

Acknowledgment. This research was supported by a grant from the National Institutes of Health, GM-26226. We are indebted to J. D. Satterlee for numerous helpful discussions.

(60) Chacko, V. P.; La Mar, G. N. *J. Am. Chem. Soc.* **1982**, *104*, 7002–7007.

(61) Sitter, A. J.; Reczec, C. M.; Terner, J. *J. Biol. Chem.* **1985**, *260*, 7515–7522.